Virtual electrodes generated by focused penta-polar current stimulation for neuromodulation

Shinyong Shim[1,2], *Jeong Hoan Park*[3], *Sung June Kim*[1,2,4] ✉

[1]*Department of Electrical and Computer Engineering, Seoul National University, Seoul 08826, Republic of Korea*
[2]*Inter-University Semiconductor Research Center, Seoul National University, Seoul 08826, Republic of Korea*
[3]*Department of Electrical and Computer Engineering, National University of Singapore, Singapore 119077, Singapore*
[4]*Institute on Aging, Seoul National University, Seoul 08826, Republic of Korea*
✉ *E-mail: kimsj@snu.ac.kr*

Published in Micro & Nano Letters; Received on 31st May 2019; Revised on 31st December 2019; Accepted on 31st January 2020

Virtual electrodes in neuromodulation can provide more delicate stimulation patterns with a limited number of physical electrodes in a confined area. Many researchers successfully verified the effectiveness of virtual electrodes in clinical trials, using current steering, which modulates electric fields produced by multi-polar stimulation. Still, it is questioned how these virtual electrodes are really generated in an electrolyte, especially in two dimensions. In order to answer this question, this work analyses the virtual electrode generation by comparing finite element analysis and in vitro evaluation of penta-polar stimulation. Penta-polar stimulation was realised using custom-designed integrated circuits and electrodes with an individual diameter of 450 μm and a centre-to-centre spacing of 800 μm. The customised test setup of electric field measurement estimated (i) the focused electric fields by the penta-polar stimulation and (ii) the optimum distance from the electrodes, at which virtual electrodes were most effectively generated. Compared with mono-polar stimulation, the penta-polar stimulation showed 0.594 and 0.545 times smaller electric field distribution areas, respectively, at a distance from the electrodes of 100 μm. Furthermore, the virtual electrodes showed the best performance at a distance from the electrodes of 150 μm, while the distance varied from 13 to 250 μm.

1. Introduction: Neuromodulation, which involves electrical stimulation to evoke neural activities, has been widely applied to prostheses restoring impaired neural functions. In neural prostheses, electrodes are essential components for delivering stimuli to target neurons. To generate delicate stimulation patterns, these electrodes have been developed with smaller size and higher density by the help of breakthroughs in microfabrication [1].

These improvements have helped researchers to stimulate a dense network of neurons in a confined space, such as in the cochlea, in the retina, or in the brain cortex [2–5]. However, even if electrodes become sufficiently small, it is demanding to arrange them to precisely stimulate individual neurons. Electric crosstalk, the spatial superposition of electric fields (E-fields), among dense electrodes leads interactions between simultaneous stimuli and degrades independence of every single electrode [6–8]. Hence, adequate spacing between adjacent electrodes is required, and this causes a limited number of physical electrodes, which hinders precise stimulation.

Many researchers have proposed stimulation strategies using virtual electrodes to overcome these limitations [3, 8–10]. Virtual electrodes are intermediate areas with large magnitudes of E-fields between physical electrodes. Such virtual electrodes can be generated by current steering, which is an approach to combine stimuli supplied from two or more adjacent physical electrodes simultaneously; this approach thereby can modulate the distribution of E-fields made by multi-polar stimulation as shown in Fig. 1.

The feasibility and effectiveness of virtual electrodes in vivo have been verified through clinical trials and animal tests for cochlear implants and retinal prostheses, respectively [11, 12]. In these research studies, virtual electrodes induced additional pitch perception in adult cochlear implant recipients and effectively altered neural activation patterns in the visual cortex. Nevertheless, to the best of our knowledge, there have been no studies on how virtual electrodes are generated in an electrolyte, according to an amplitude ratio between the stimuli of two adjacent physical electrodes and a distance from the physical electrodes. Therefore, in this study, we aimed to evaluate the virtual electrode generation in vitro, especially in two dimensions, where stimulation on the retina or the brain cortex is closely related. In addition, finite element analysis (FEA) in the same conditions with this in vitro evaluation was carried out as well, in order to prove the relationship between FEA and in vitro evaluation results.

For virtual electrode generation, a configuration of physical electrodes is crucial to spatial E-field distribution. Such a configuration in two dimensions can have a variety of arrangements including a grid shape or a honeycomb shape [11, 12]. Among these shapes, we chose the grid-shaped configuration because it consists of one centre electrode and four peripheral electrodes, which can be driven at the same time with lower power than the honeycomb-shaped configuration using one centre electrode and six peripheral electrodes; we thus used a penta-polar stimulation strategy with current steering.

To realise penta-polar stimulation, application-specific integrated circuits (ASICs) for such stimulation and polymer-based electrodes arranged in a cross shape, a specific portion of grid shape, were designed. The effectiveness of penta-polar stimulation on focusing E-fields was evaluated first through comparison with mono-polar stimulation. Furthermore, changes of the E-fields were estimated from both FEA and in vitro evaluation in accordance with an amplitude ratio between the stimuli of two adjacent electrodes and a distance from the electrodes.

2. Penta-polar stimulation ASIC: As described in Fig. 2*a*, we designed a penta-polar stimulation ASIC consisting of five biphasic current sources and 16 output channels, using the AMS 0.35 μm high-voltage complementary metal oxide semiconductor (CMOS) process. Details of the designed penta-polar stimulation ASIC are demonstrated in Table 1. The designed ASIC received pulse width modulated (PWM) data carried by a frequency of 6.25 MHz. These PWM data were transferred to a data receiver and a digital controller in the designed ASIC. The data receiver enveloped the data to become a clock signal needed for operating

doi: 10.1049/mnl.2019.0348

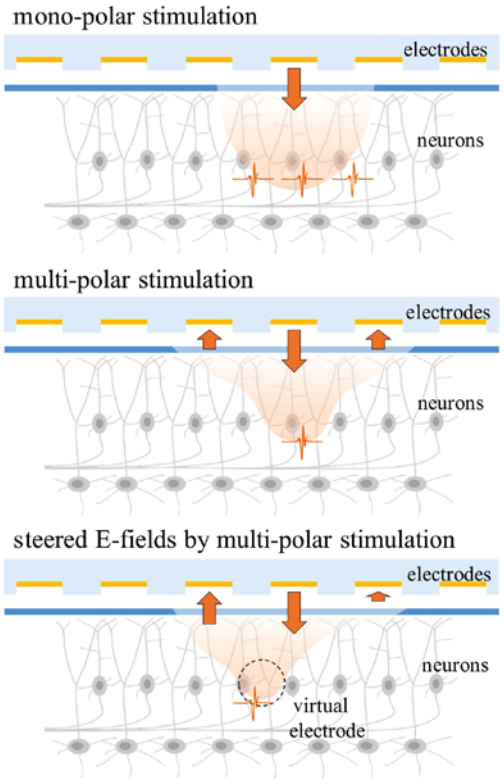

Fig. 1 *Schematic diagrams of E-field distribution: mono-polar stimulation (top), multi-polar stimulation (middle), and multi-polar stimulation with current steering (bottom)*

Table 1 Details of the designed penta-polar stimulation ASIC

Process		AMS 0.35 µm high-voltage CMOS
die size, mm		4.5 × 2.4
operating voltage, V		3.3–9
stimulation parameters	amplitude, mA	0.01–1.00
	duration, ms	0.05–3.20
	pulse interval, ms	0.80–51.2

the digital controller. The digital controller then counted the number of pulses in the data and demodulated them into corresponding bit streams. Using these bit streams, the digital controller controlled overall functions of the designed ASIC: changing the parameters of five biphasic current pulses and activating output channels where the pulses were to be supplied. Each biphasic current pulse was supplied from an independent source so as not to interact with other pulses at the same time.

The operation of simultaneous stimulation was verified as shown in Fig. 2*b*. For measurements, the load resistance of 10 kΩ was connected to each output channel. The parameters of each biphasic current pulse were arbitrarily determined only for this verification, as listed in Table 2.

3. FEA and in vitro evaluation: A simple finite element model was constructed to simulate spatial E-field distribution made by penta-polar stimulation. The high-frequency structure simulator from ANSYS was utilised for this FEA. First, five stimulation electrodes with an individual diameter of 450 µm and a centre-to-centre spacing of 800 µm were designed and arranged in a cross shape; the following references were used to determine these dimensions [12–14] because the references showed neural activation patterns altered by current steering in vivo using

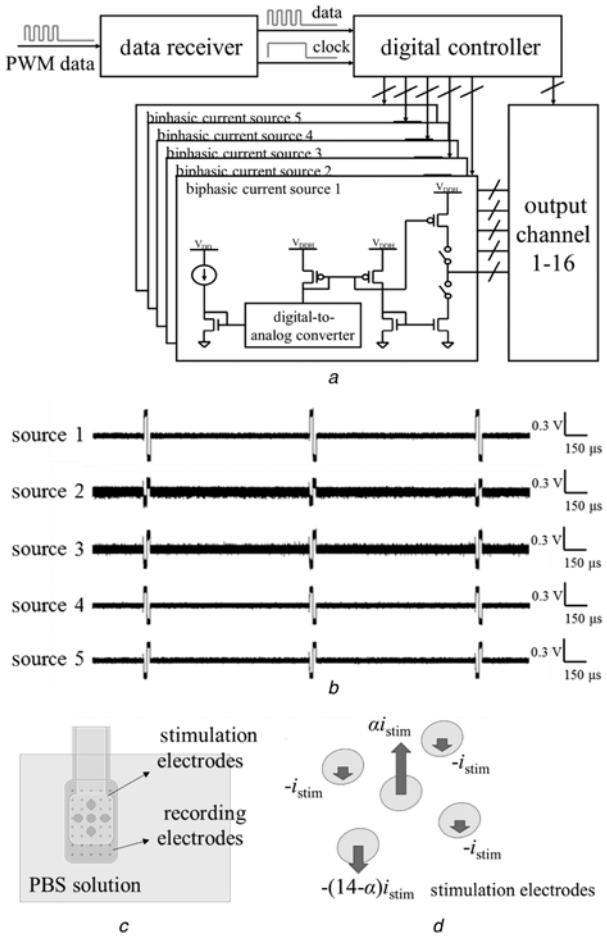

Fig. 2 *Designed penta-polar stimulation ASIC and in vitro evaluation setup of E-field measurement in a PBS solution*
a Schematic of the designed ASIC
b Five biphasic current pulses supplied from the designed ASIC at the same time
c Illustration of the in vitro evaluation setup
d Schematic diagram showing an amplitude ratio between the simultaneous stimuli during penta-polar stimulation for virtual electrode generation

Table 2 Parameters of biphasic current pulses for verifying the operation of the designed penta-polar stimulation ASIC (Fig. 2*b*)

duration, ms		0.05
pulse interval, ms		0.80
amplitude, mA and phase	source 1	0.03 and anodic-first
	source 2	0.01 and cathodic-first
	source 3	0.02 and cathodic-first
	source 4	0.02 and anodic-first
	source 5	0.02 and cathodic-first

electrodes with similar dimensions. An electrode material was 100 nm thick gold and a substrate material was a 50 µm-thick cyclic olefin polymer (COP). Both materials were chosen because electrodes based on them can be simply fabricated using the process developed in our previous study [15]. Additionally, an ambient condition around the electrodes was filled with phosphate buffered saline (PBS) solution, as an electrolyte, in order to mimic in vivo environments.

In addition to the FEA, an in vitro evaluation setup similar to that of the FEA was also built as depicted in Fig. 2*c*. The designed stimulation electrodes were fabricated using COPs (ZF14 and ZF16, Zeon Corporation, Japan) and thin gold films (Hanil Gold Leaf Co., Korea) by thermal lamination and laser machining [15].

An averaged impedance of the stimulation electrodes was measured to be 2.23 kΩ at 1 kHz by an impedance analyser (SI 1287 and SI 1260, Solartron Analytical, UK). Measurements were conducted in a PBS solution (Gibco #10,010, Invitrogen Life Technologies, USA). Unlike the FEA, recording electrodes were required for in vitro evaluation. These recording electrodes were made to be an 8×5 array on a gold-plated printed circuit board. The recording electrodes featured an individual diameter of 75 µm and a centre-to-centre spacing of 500 µm. From measurements, electric potentials were garnered using an oscilloscope (DPO4034, Tektronix, Inc., USA). Therefore, measured electric potentials should be converted into E-fields by

$$E = |-\nabla V| \tag{1}$$

where E is the E-field magnitude and V is the electric potential; thereby the spatial E-field distribution was obtained.

In both FEA and in vitro evaluation, the effectiveness of penta-polar stimulation on focusing E-fields was evaluated by comparing with mono-polar stimulation prior to the virtual electrode generation. E-field magnitudes were simulated and measured at a distance from the stimulation electrodes of 100 µm. In mono-polar stimulation, current pulses with an amplitude of 120 µA were supplied from the centre electrode and flowed to a distant return electrode, located around 2 cm away from the stimulation electrodes in the same plane. In contrast, in penta-polar stimulation, current pulses with the same amplitude were supplied from the centre electrode and divided into four to be flowed to the peripheral electrodes, respectively.

Subsequently, changes of E-field distribution while varying an amplitude ratio between the stimuli of two adjacent stimulation electrodes were also estimated to localise virtual electrodes. This estimation was conducted at distances of 13, 50, 100, 150, 200, and 250 µm, respectively. The amplitude ratio of the stimuli was varied as described in Fig. 2*d*. The amplitude of the fundamental current i_{stim} was set to be 10 µA, and the amplitude ratio coefficient α was changed to be 1, 3, 5, 7, 9, 11, and 13, respectively, with increments of 20 µA using the ASIC. The maximum amplitude of 130 µA was determined not to exceed one half of the water window level of 0.6 V safely, with the averaged electrode impedance. In all cases, the duration and pulse interval were set to be 0.05 and 0.80 ms, respectively, with the maximum charge density of 4.09 µC/cm^2, which was a lot lower than non-damaging, safe levels of stimulation [16]. During the evaluations, a distant return electrode was located around 2 cm away from the stimulation electrodes in the same plane. After simulating and measuring E-field magnitudes, the weighted centroids of the magnitudes, which were considered as virtual electrodes, from both FEA and in vitro evaluation results were plotted as neural activation patterns evoked by current steering were analysed in the previous research [12].

4. Results and discussion: E-fields produced by mono-polar and penta-polar stimulation are shown in Fig. 3. Each result of the FEA and the in vitro evaluation was normalised using the maximum E-field magnitude measured from the FEA and in vitro evaluation, respectively. Overall E-field magnitudes of penta-polar stimulation were slightly lower than those of mono-polar stimulation, but field distribution areas were smaller in penta-polar stimulation than in mono-polar stimulation. To analyse these field distribution areas quantitatively, we assumed that effective E-fields had the magnitudes of >20% of the maximum value. As a result, compared with mono-polar stimulation, penta-polar stimulation showed 0.594 and 0.545 times smaller areas of field distribution, respectively, at the distance from the stimulation electrodes of 100 µm.

Furthermore, the weighted centroids of E-field magnitudes according to the distance were plotted in Fig. 4, while varying the amplitude ratio coefficient (Fig. 2*d*). These results on virtual

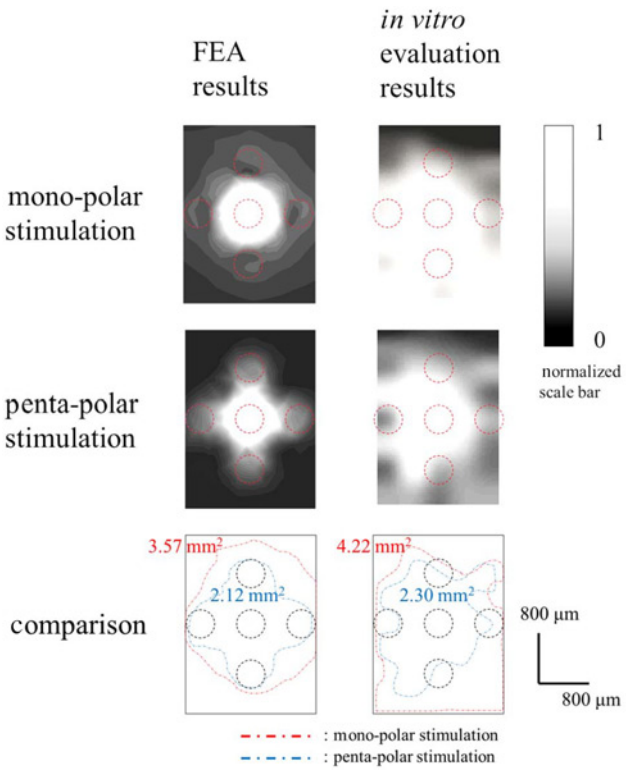

Fig. 3 *E-fields simulated and measured from the FEA and in vitro evaluation, respectively, with comparison results between mono-polar and penta-polar stimulation*

electrode generation were estimated qualitatively, as there could be slight differences between the FEA and the in vitro evaluation results due to the presence of the recording electrodes. At the distance of <100 µm, the weighted centroids were created near the edge of each electrode. The weighted centroids were generated most effectively at a distance of 150 µm. The greatest number of weighted centroids between two adjacent stimulation electrodes was observed at the distance of 100 µm, but more linear arrangements of them were produced at the distance of 150 µm. In contrast, at the farther distance than 150 µm, the number of weighted centroids between two stimulation electrodes decreased, and the arrangements became non-linear again. In addition, the weighted centroids tended to be created around the middle of each electrode as the distance increased.

In this study, we verified the effectiveness of focused penta-polar current stimulation and virtual electrodes generated by such stimulation. Although both results of the FEA and in vitro evaluation did not exactly coincide due to the differences such as the presence of the recording electrodes, they showed the same information on the tendency of focusing E-fields and virtual electrode generation as evaluated above. This also indicates that FEA can be sufficient to confirm only the tendency, but in vitro evaluation is highly required for precise stimulation using virtual electrodes in practice.

From the results, especially the fact that virtual electrodes demand a certain distance from physical electrodes was proven. In this case, such a distance was about 150 µm. This distance must be considered in design procedures of stimulation electrodes for precisely steering virtual electrodes. For example, the thickness of a passivation layer of stimulation electrodes can be adjusted to be identical to the distance or a medium such as a hydrogel can be placed between target neurons and stimulation electrodes to match the distance. On the other hand, the distance can be used for activating neurons in different depths or layers. For this purpose, it is thought that neural stimulation using virtual electrodes

doi: 10.1049/mnl.2019.0348

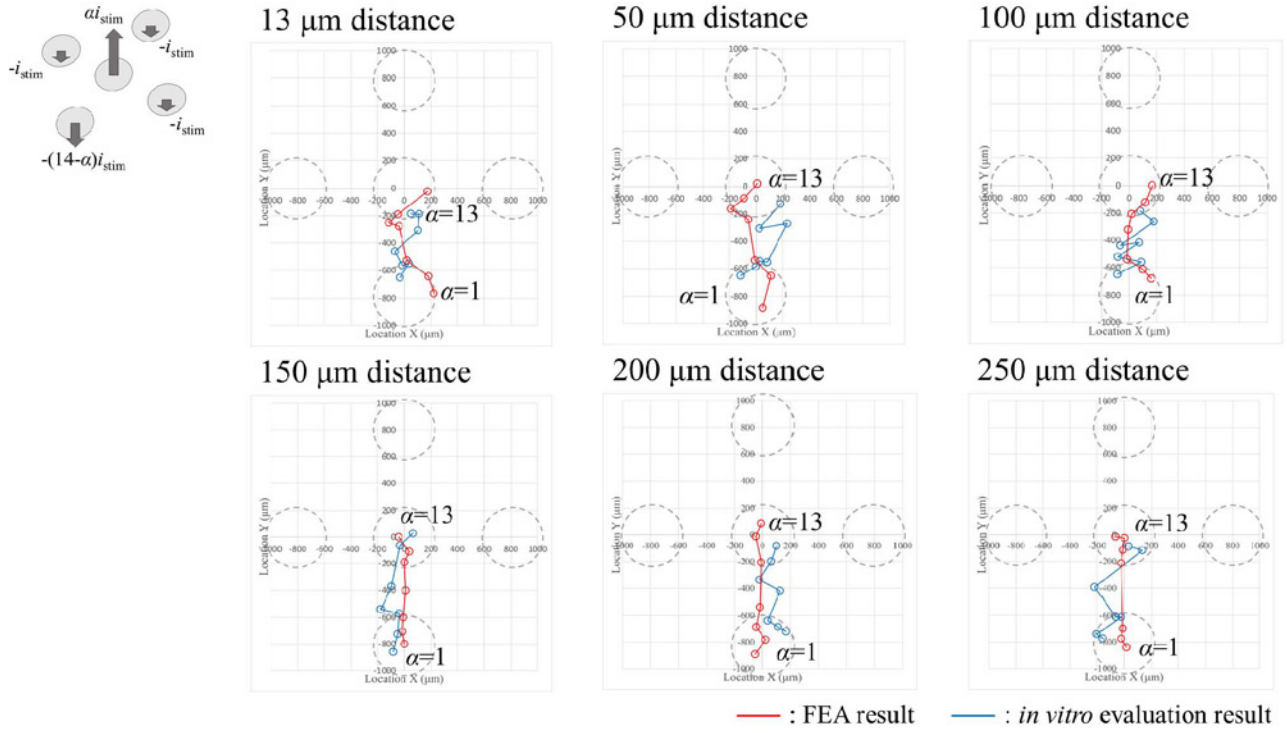

Fig. 4 *Weighted centroids of E-field magnitudes, virtual electrodes, plotted from both FEA and in vitro evaluation results in accordance with the distance, while varying an amplitude ratio between the stimuli of two adjacent stimulation electrodes (x-axis: location X, μm and y-axis: location Y, μm)*

can be performed in a deeper or shallower layer than 150 μm by changing configurations of the stimulation electrodes.

Herein, we only discussed the results of penta-polar stimulation with the specifically designed stimulation electrodes in a PBS solution. Therefore, further studies on virtual electrode generation would be required for different configurations of physical electrodes with neural tissue models in the future.

5. Conclusion: In this Letter, we reported virtual electrodes generated by focused penta-polar current stimulation for neuromodulation. Our purpose was to apply virtual electrodes in two dimensions, thus the penta-polar stimulation ASICs and the stimulation electrodes arranged in a cross shape were designed. The effectiveness of penta-polar stimulation was evaluated by comparing it with mono-polar stimulation. Furthermore, virtual electrodes were estimated in accordance with a distance from the electrodes, while varying an amplitude ratio of the simultaneous stimuli. In conclusion, we verified the effectiveness and found the distance-dependency of the virtual electrode generation using penta-polar stimulation.

6. Acknowledgments: This work was supported in part by a grant to CABMC funded by the Defense Acquisition Program Administration (grant no. UD170030ID) and in part by the Samsung Electronics Corp (grant no. 5264-20180116). In addition, the EDA tool was supported by the IC Design Education Center (IDEC), Korea.

7 References

[1] Cogan S.F.: 'Neural stimulation and recording electrodes', *Annu. Rev. Biomed. Eng.*, 2008, **10**, pp. 275–309

[2] Wise K.D., Bhatti P.T., Wang J., *ET AL.*: 'High-density cochlear implants with position sensing and control', *Hearing Res.*, 2008, **242**, (1–2), pp. 22–30

[3] Bonham B.H., Litvak L.M.: 'Current focusing and steering: modeling physiology and psychophysics', *Hearing Res.*, 2008, **242**, (1–2), pp. 141–153

[4] Viventi J., Kim D.H., Vigeland L., *ET AL.*: 'Flexible, foldable, actively multiplexed, high-density electrode array for mapping brain activity in vivo', *Nat. Neurosci.*, 2011, **14**, (12), pp. 1599–1605

[5] Mathieson K., Loudin J., Goetz G., *ET AL.*: 'Photovoltaic retinal prosthesis with high pixel density', *Nat. Photonics*, 2012, **6**, (6), pp. 391–397

[6] Wilke R.G., Greppmaier U., Stingl K., *ET AL.*: 'Fading of perception in retinal implants is a function of time and space between sites of stimulation', *Invest. Ophthalmol. Vis. Sci.*, 2011, **52**, (14), p. 458

[7] Wilke R., Gabel V.P., Sachs H., *ET AL.*: 'Spatial resolution and perception of patterns mediated by a subretinal 16-electrode array in patients blinded by hereditary retinal dystrophies', *Invest. Ophthalmol. Vis. Sci.*, 2011, **52**, (8), pp. 5995–6003

[8] Moghaddam G.K., Lovell N.H., Wilke R.G., *ET AL.*: 'Performance optimization of current focusing and virtual electrode strategies in retinal implants', *Comput. Methods Programs Biomed.*, 2014, **117**, (2), pp. 334–342

[9] Berenstein C.K., Mens L.H., Mulder J.J., *ET AL.*: 'Current steering and current focusing in cochlear implants: comparison of monopolar, tripolar, and virtual channel electrode configurations', *Ear Hearing*, 2008, **29**, (2), pp. 250–260

[10] Martens H.C.F., Toader E., Decré M.M.J., *ET AL.*: 'Spatial steering of deep brain stimulation volumes using a novel lead design', *Clin. Neurophysiol.*, 2011, **122**, (3), pp. 558–566

[11] Firszt J.B., Koch D.B., Downing M., *ET AL.*: 'Current steering creates additional pitch percepts in adult cochlear implant recipients', *Otol. Neurotol.*, 2007, **28**, (5), pp. 629–636

[12] Dumm G., Fallon J.B., Williams C.E., *ET AL.*: 'Virtual electrodes by current steering in retinal prostheses', *Invest. Ophthalmol. Vis. Sci.*, 2014, **55**, (12), pp. 8077–8085

[13] Wong Y.T., Dommel N., Preston P., *ET AL.*: 'Retinal neurostimulator for a multifocal vision prosthesis', *IEEE Trans. Neural Syst. Rehabil. Eng.*, 2007, **15**, (3), pp. 425–434

[14] Matteucci P.B., Chen S.C., Tsai D., *ET AL.*: 'Current steering in retinal stimulation via a quasimonopolar stimulation paradigm', *Invest. Ophthalmol. Vis. Sci.*, 2013, **54**, (6), pp. 4307–4320

[15] Shim S., Park H.Y., Choi G.J., *ET AL.*: 'A simply fabricated neural probe by Laser machining of a thermally laminated gold thin film on transparent cyclic olefin polymer', *ACS Omega*, 2019, **4**, (2), pp. 2590–2595

[16] Cogan S.F., Garrett D.J., Green R.A.: 'Electrochemical principles of safe charge injection' (John Wiley & Sons, Hoboken, NJ, USA, 2016)